

Rotational excitation in two-center Coulomb-scattering systems: Application to electron-molecule collisions

A. Ernesti

Department of Chemistry, University of Durham, South Road, Durham DH1 3LE, England

M. Gote and H. J. Korsch

Fachbereich Physik, Universität Kaiserslautern, D-67653 Kaiserslautern, Germany

(Received 1 March 1995)

Rotational excitation in electron-diatomic-molecule collisions at intermediate collision energies ($\sim 10^2$ eV) is discussed within a quantum-mechanical two-center model using a Coulomb-scattering approximation. Rotational rainbow effects are discussed, in particular for heteronuclear diatomic molecules. The model is applied to collisional excitation of HCl and CO as well as to the homonuclear cases N_2 and Cl_2 . The model predictions are compared with recent experimental results as well as with elaborate numerical computations for the homonuclear systems.

PACS number(s): 34.80.Gs, 34.50.Ez

I. INTRODUCTION

In previous articles the rotational excitation of diatomic molecules by collisions with electrons at about 10^2 eV has been studied for the case of Na_2 molecules, where state-to-state differential cross sections have been experimentally determined [1,2]. The most prominent feature of these cross sections is the pronounced rotational rainbow structure, i.e., a characteristic maximum, the "rotational rainbow," accompanied by oscillations ("rotational rainbow oscillations"). This is found in the rotational distributions at fixed scattering angle as well as in the angular dependence of the inelastic cross sections as discussed in the recent reviews [3,4] on rotational rainbow effects in atom-molecule or electron-molecule scattering.

For Na_2 , the experimental results could be compared with quite elaborate theoretical computations based on the fixed-nuclei approximation including, e.g., electron exchange (see [1,5,6] for details) in very good agreement with the measurements. In addition, it turned out that a very simple two-center scattering model was capable of describing the rotational state-to-state cross sections surprisingly accurately [6,7] (see also the discussion in [3]). The two-center model was then extended to vibrationally excited molecules [8–10], again in good agreement with the experiment for Na_2 [8], as well as to rotational excitation of polyatomic molecules [3,11–13], where no experimental state-to-state differential cross sections have been reported up to now.

Because of the restriction of the previous studies to Na_2 molecules, it is of interest to analyze different systems. In this work we report on such a study for two homonuclear diatomic molecules, N_2 and Cl_2 , and for two heteronuclear ones, HCl and CO, where experimental measurements have been carried out very recently. Section II gives a short outline of the two-center scattering model emphasizing the effects due to heteronuclear molecules. The comparison of the model with recent ex-

periments (described in Sec. III) and more elaborate theoretical results is discussed in Sec. IV.

II. COULOMB-SCATTERING SPECTATOR MODEL

The two-center scattering model for rotational excitation of diatomic molecules [3,6,7] has been successfully applied to Na_2 targets at intermediate energies [1,2,6,8]. For molecules not vibrationally excited initially, it has been demonstrated that the rotational excitation of the target can be well described within the rigid rotor approximation, where the distances of the molecular atoms from the scattering center are fixed at their equilibrium values. The collision is treated as vibrationally elastic. This collision model has been discussed quite extensively in previous articles [3,7] and a number of useful analytic formulas has been derived. Here we give a short outline of those results, which are important for an application to heteronuclear molecules, in particular within the Coulomb-interaction approximation.

The scattering of the (fast) electron is approximated by an impulsive collision with only one of the molecular atoms, where the interaction is moreover approximated by a simple potential scattering. The collision is assumed to be (energetically) elastic, $|\vec{k}'| \approx |\vec{k}| = k$, and the momentum transfer is

$$\Delta k = |\vec{k}' - \vec{k}| \approx 2k \sin(\vartheta/2), \quad (1)$$

where ϑ is the scattering angle.

Since for diatomic targets the cross sections for the excitation of initially excited molecules may be calculated from $j \leftarrow 0$ cross sections using a well-known factorization formula [7,14], in the present study we confine ourselves to molecules initially in the rotational ground state. The experimentally not resolved m transitions

have been summed and thus the differential cross section is given by

$$\frac{d\sigma}{d\Omega}(j \leftarrow 0|\vartheta) = \left| F_j^{(1)}(\vartheta) f^{(1)}(\vartheta) + (-1)^j F_j^{(2)}(\vartheta) f^{(2)}(\vartheta) \right|^2, \quad (2)$$

where the form factor $F_j^{(\nu)}(\vartheta)$ for rotational transitions $0 \rightarrow j$ is given by the simple expression

$$F_j^{(\nu)}(\vartheta) = \sqrt{2j+1} j_j(\Delta_\nu), \quad \nu = 1, 2. \quad (3)$$

Here, j_j is the spherical Bessel function and its argument is the momentum transfer multiplied by the distance of the atom ν from the center of mass:

$$\Delta_\nu = r_\nu \Delta k = 2r_\nu k \sin(\vartheta/2) \quad (4)$$

(note that $r_2/r_1 = m_1/m_2$, where $m_1 \geq m_2$ are the masses of the molecular atoms).

In addition, the differential cross sections (2) depend on the elastic scattering amplitudes $f^{(\nu)}(\vartheta) = |f^{(\nu)}| e^{i\phi_\nu}$ for collisions with atom ν .

The two-center scattering model can be extended to N -center scattering describing collisional excitation of polyatomic molecules. Furthermore, it may be of interest to note that the model shows a close similarity to the Born-type approximation developed for inelastic electron-atom scattering at high energies (see, e.g., [15, Sec. 145] or [16, Sec. 4.3]).

The rotational excitation of homonuclear molecules has been studied quite extensively for Na_2 [7], where the elastic scattering amplitude $f(\vartheta)$ has been determined by fitting a screened Coulomb potential

$$V(r) = \frac{z}{r} [(1-a)e^{-br} + ae^{-cr}] \quad (5)$$

to numerical data for the electron- Na_2 interaction [z is the number of protons of the target atom; atomic units are used in Eq. (5)]. Such a description of the interaction is of essential importance if one is actually interested in the *angular* dependence of the differential cross sections. Here, we will only discuss the rotational transition probabilities $P(j \leftarrow 0|\vartheta)$ at fixed scattering angle, i.e.,

$$\frac{d\sigma}{d\Omega}(j \leftarrow 0|\vartheta) = P(j \leftarrow 0|\vartheta) \left. \frac{d\sigma}{d\Omega}(\vartheta) \right|_{\text{tot}}. \quad (6)$$

We further note that the total (j summed) differential cross section can be evaluated in closed form [7] using the addition theorem of the spherical Bessel functions, which yields

$$\begin{aligned} \left. \frac{d\sigma}{d\Omega}(\vartheta) \right|_{\text{tot}} &= \sum_j \frac{d\sigma}{d\Omega}(j \leftarrow 0|\vartheta) \\ &= |f^{(1)}(\vartheta)|^2 + |f^{(2)}(\vartheta)|^2 \\ &\quad + 2|f^{(1)}(\vartheta)f^{(2)}(\vartheta)| \frac{\sin \Delta_0}{\Delta_0} \cos(\phi_1 - \phi_2) \end{aligned} \quad (7)$$

with $\Delta_0 = \Delta_1 + \Delta_2 = d \Delta k$ ($d = r_1 + r_2$ is the intermolecular distance).

The influence of the electron-atom potential on the normalized transition probabilities at fixed ϑ is less important [note, for instance, that $P(j \leftarrow 0|\vartheta)$ is *independent* of the interaction potential for homonuclear molecules] and we therefore include only the dominant term of the interaction potential at short range, the Coulomb part. Using the fact that the Coulomb-scattering amplitude is proportional to the nuclear charge number, $f^{(\nu)} \sim z_\nu$, we obtain our working equation

$$P(j \leftarrow 0|\vartheta) = P_M(j \leftarrow 0|\vartheta) + P_I(j \leftarrow 0|\vartheta) \quad (8)$$

with the main contribution

$$P_M(j \leftarrow 0|\vartheta) = (2j+1) \frac{z_1^2 j_j^2(\Delta_1) + z_2^2 j_j^2(\Delta_2)}{z_1^2 + z_2^2 + 2z_1 z_2 \frac{\sin \Delta_0}{\Delta_0} \cos(\phi_1 - \phi_2)} \quad (9)$$

and the interference term

$$P_I(j \leftarrow 0|\vartheta) = (-1)^j 2(2j+1) \times \frac{z_1 z_2 j_j(\Delta_1) j_j(\Delta_2) \cos(\phi_1 - \phi_2)}{z_1^2 + z_2^2 + 2z_1 z_2 \frac{\sin \Delta_0}{\Delta_0} \cos(\phi_1 - \phi_2)}. \quad (10)$$

Here, ϕ_1 and ϕ_2 are the Coulomb-scattering phase shifts (see, e.g., [15, Sec. 133])

$$\phi_\nu = 2 \left\{ \frac{z_\nu}{ka_0} \ln[\sin(\vartheta/2)] - \arg \left[\Gamma \left(1 + i \frac{z_\nu}{ka_0} \right) \right] \right\} \quad (11)$$

(a_0 is the Bohr radius).

It is instructive to analyze the rotational excitation in a classical model as discussed for homonuclear targets in [3,7]. Here, the corresponding classical rotational distribution is given by

$$P_C(J \leftarrow 0|\vartheta) = \frac{z_1^2}{z_1^2 + z_2^2} P_C^{(1)}(J \leftarrow 0|\vartheta) + \frac{z_2^2}{z_1^2 + z_2^2} P_C^{(2)}(J \leftarrow 0|\vartheta) \quad (12)$$

with

$$P_C^{(\nu)}(J \leftarrow 0|\vartheta) = \begin{cases} \frac{J}{J_R^{(\nu)} \sqrt{(J_R^{(\nu)})^2 - J^2}}, & J < J_R^{(\nu)} \\ 0, & J > J_R^{(\nu)} \end{cases} \quad (13)$$

and $J = j + 1/2$. The classical cross sections diverge at the rotational rainbows $J_R^{(\nu)} = \Delta_\nu$ [3]. For heteronuclear targets, two rainbows appear at $J_R^{(1)} < J_R^{(2)}$, where the first one, $J_R^{(1)}$, is due to scattering from the heavier atom (mass $m_1 \geq m_2$) of the molecule. Rotational excitation of $J > J_R^{(2)}$ is classically forbidden.

Semiclassically, these rainbows are accompanied by so-called rotational rainbow oscillations [3] on the classically allowed side (the "bright" side of the rainbow), which ap-

pear in the quantum cross sections (8) as oscillations in the spherical Bessel functions. In addition, we observe interference terms of both rainbows, oscillating because of the phase mismatch $\phi_1 - \phi_2$ of the Coulomb-scattering phases. The importance of this interference term is discussed in more detail below.

III. EXPERIMENTAL SETUP AND EVALUATION PROCEDURE

The measurements have been performed with a newly designed high-resolution electron spectrometer of crossed-beam type. An almost monochromatic electron beam, produced in a revolving electron gun, is crossed perpendicularly with an effusive target gas beam. The scattered electrons are detected in an electron analyzer with acceptance half angles of 3° . The electron gun and electron analyzer are of identical structural form and size. Tandem hemispherical condensers are used for energy selection. The electron optics is computer controlled for better handling and improved stability. Both systems are differentially pumped to a pressure smaller than 10^{-7} mbar during operation. All components of the spectrometer are made from stainless steel. To achieve undisturbed surfaces and homogeneous electron work functions they were electropolished after fabrication. During all measurements the overall energy resolution (electron gun, analyzer, and Doppler broadening) of the spectrometer was 10–12 meV (full width at half maximum), and the beam current about 10^{-10} A.

A rather high energy resolution is necessary since the information about the rotational excitation is extracted from a line-shape analysis of the rotationally broadened energy loss spectra. An unbroadened reference apparatus profile is obtained by electron scattering from rare gas atoms under identical scattering conditions for each energy and angle. State-to-state rotational transition cross sections have been deconvoluted as was proposed by Shimamura [17]. The formalism, developed for linear and spherical-top molecules, is based on the adiabatic nuclei rotation approximation, which is very well fulfilled in the present case. This formalism was extended to take care of the Doppler effect. Much emphasis was laid on robust numerical algorithms.

A detailed discussion of the experiment may be found in Refs. [18,19].

IV. EXPERIMENTAL RESULTS AND THEORETICAL ANALYSIS

Elastic collisions of fast electrons with atoms are well described within the Born approximation. The prerequisite for such a simple description is that the electronic projectiles are faster than the electrons of the target atom. Applying Born's method leads to an integral over the charge distribution of the target atom. The contribution from the nucleus turns out to be proportional to the number of its protons, whereas the atomic electrons

contribute proportionally to the Fourier transform of the electron density. However, it can be shown that the latter is negligible for a large momentum transfer, i.e.,

$$a_0 \Delta k \gg 1 \quad (14)$$

(see, e.g., [15, Sec. 139]), where a_0 is Bohr's radius. For electron-molecule collisions, this condition limits the use of the Coulomb-scattering spectator model derived in Sec. II.

For backward scattering and high collision energies such as 500 and 1000 eV, the value of $a_0 \Delta k$ equals 12.1 and 17.1, respectively, and thus in this high-energy region the condition (14) has been found to be well fulfilled (see also the discussion below). The transition probabilities of two high-energy collisions by CO are shown in Fig. 1. As discussed in Sec. II, the classical distribution possesses a double rainbow structure. For backward scattering and a collision energy of 500 eV, the two classical square-root rainbow singularities are found at $j = 10.58$ and 14.26 . The first rainbow corresponds to the oxygen atom and the second one to the carbon atom. For both energies, at the bright sides of the rainbows the quantum rainbow patterns show two quite pronounced maxima and a few less intensive maxima called rainbow oscillations. At the dark side of the rainbow singularities the quantum patterns decrease exponentially. As discussed above, both quantum distributions can be expected to give quite good predictions of the realistic cross sections at these high energies.

For lower impact energies such as 100 eV at the fixed scattering angle of 120° , the value of $a_0 \Delta k$ is just smaller than 5 and the Coulomb approximation of the electron-atom interaction seems to break down. However, as has been shown in previous work [6,7,11], for homonuclear targets the transition probabilities are independent of the

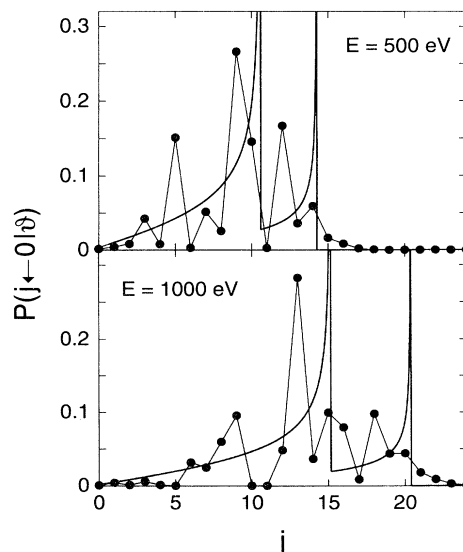


FIG. 1. Quantum (•) and classical (—) transition probabilities of the rotational excitation of CO from its rotational ground state for electron backward scattering at 500 and 1000 eV.

electron-atom cross section. Since in this particular case $z_1 = z_2$ and $\phi_1 = \phi_2$, this may be seen from the equations given in Sec. II, which simplify to the equations discussed in Ref. [7]. Thus, in the case of homonuclear targets, the rotational excitation probability depends on the molecular form factor, which for diatomic molecules is only a function of the internuclear distance d .

Previously, the homonuclear spectator model has been found to provide an excellent description for electron- Na_2 collisions at intermediate energies and large scattering angles [1,2,6,8]. For N_2 and Cl_2 , the results of the spectator model are compared with experimental results by Gote [18] and close-coupling calculations by Kutz [20,21] in Fig. 2. The rainbow pattern predicted by the two-center spectator model is in very good agreement both with the close-coupling and with the experimental results, which demonstrates that this simple model can also successfully describe rotational excitation of molecules different from Na_2 . As expected, for large scattering angles such as 160° all distributions agree well and pronounced maxima appear at the bright sides of the classical rainbows close to their singularities. Surprisingly, this agreement holds for small angles such as 10° as well. In this case, the scattering angle is so small that the classical rainbow position J_R is below $1/2$ and since $j = J - 1/2$ it gets shifted below $j = 0$. Therefore no classical distribution is drawn for $\vartheta = 10^\circ$. For both targets, at such small scattering angles the spectator model predicts rotationally elastic collisions again in excellent agreement with experiments and close-coupling calculations.

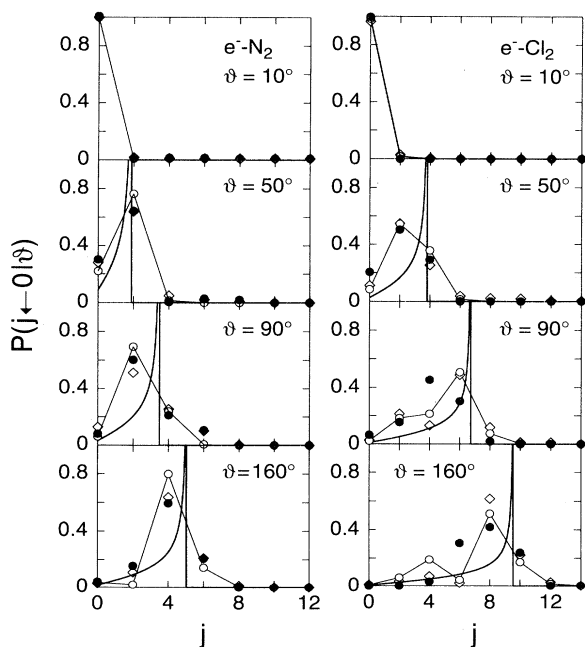


FIG. 2. Rotational rainbow distributions for electron- N_2 and Cl_2 at 100 eV and four fixed scattering angles ϑ . Results from close-coupling calculations (\diamond) and from the spectator model ($\text{---}\circ\text{---}$) are compared with the experimental results (\bullet). Also shown is the distribution (---) from a classical spectator model.

Note that, since the rotational excitation of homonuclear targets is independent of the electron-atom cross section, the assumption of a Coulomb-scattering system has not been used and so in this case the condition (14) is meaningless. This is different, however, for heteronuclear molecules such as HCl and CO , where for decreasing collision energy or decreasing scattering angle the condition (14) shows the limits of the Coulomb-scattering approximation for electron scattering by atoms and molecules.

Therefore, it is instructive to discuss the quantum rainbow distribution in more detail and to distinguish the more stable or unstable features. Since the main and the interference contributions of the transition probabilities depend on the Coulomb-scattering phases, for decreasing Δk both terms are affected. However, for reasonable Δk values, the quantity Δ_0 in Eqs. (9) and (10) will still be of the order of 10^1 and thus the main contribution may be approximated as

$$P_M(j \leftarrow 0 | \vartheta) \approx (2j + 1) \frac{z_1^2 j_j^2(\Delta_1) + z_2^2 j_j^2(\Delta_2)}{z_1^2 + z_2^2} \quad (15)$$

and the interference term as

$$P_I(j \leftarrow 0 | \vartheta) \approx (-1)^j 2(2j + 1) \times \frac{z_1 z_2}{z_1^2 + z_2^2} j_j(\Delta_1) j_j(\Delta_2) \cos(\phi_1 - \phi_2). \quad (16)$$

Within this approximation, it can be seen that in first order the main contribution is independent of the phase difference $\phi_1 - \phi_2$, and thus this term turns out to be rather stable for decreasing Δk . Differently, the interference term depends still on the difference of the scattering phases ϕ_1 and ϕ_2 . For homonuclear molecules (i.e., $\phi_1 = \phi_2$), the magnitude of the interference reaches its maximum leading to the well-known selection rule of “ $\Delta j = j = \text{even}$ ” for nonvanishing probabilities. In the case of heteronuclear molecules (i.e., $\phi_1 \neq \phi_2$), the interference term is weakened into a propensity rule. The variation of the strength of the interference depends strongly on the term $\cos(\phi_1 - \phi_2)$, which is shown in Fig. 3 as a function of the scattering angle ϑ for HCl and CO . Since the charge of the Cl nucleus is much larger than the charge of either the carbon or oxygen atom, the $\cos(\phi_1 - \phi_2)$ term oscillates much faster in the HCl case. However, both figures are similar since for decreasing angle the oscillations increase (note that for CO this is not directly obvious in Fig. 3 because of the resolution for small angles).

Since the spherical Bessel function $j_j(\Delta)$ decreases exponentially for increasing j in the region $j > \Delta$, the influence of the interference disappears more or less at the dark side of the inner rainbow. At the bright side of this rainbow, the interference contribution increases the frequency of the rainbow oscillations.

From the discussion above, it is obvious that for decreasing impact energies or decreasing scattering angles a breakdown of the Coulomb-scattering approximation of the electron-atom collision shows its first evidence in the rainbow oscillation pattern at the bright side of the inner

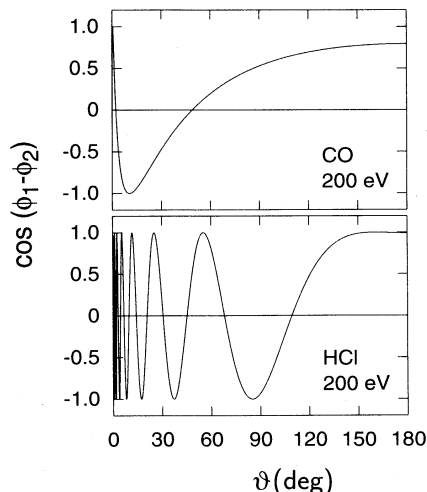


FIG. 3. Contribution of the interference term as a function of the scattering angle ϑ for HCl and CO collisions at 200 eV.

classical rainbow, whereas the outer rainbow structure is less disturbed.

Since for HCl molecules the center of mass is very close to the Cl atom, for energies of 10^2 eV the position of the inner rainbow singularity, $J_R^{(1)}$, is very close to the rotational elastic channel, whereas the outer rainbow singularity at $J_R^{(2)}$, which corresponds to the H atom, appears for large changes of the rotational angular momentum. This can be clearly seen from the ratio

$$\frac{J_R^{(1)}}{J_R^{(2)}} = \frac{r_1}{r_2} = \frac{m_2}{m_1} \approx \frac{1}{35} \ll 1. \quad (17)$$

Accordingly, electron-HCl scattering seems to be one of the best suited heteronuclear targets for a possible application of the Coulomb-scattering approximation to lower collision energies. The region of reasonable interference contributions is extremely compressed around $j = 0$. However, since the charge of the Cl nucleus is 17 times larger than the proton charge, the outer rainbow is about 300 times weaker than the inner one, as clearly shown in Fig. 4. The elastic channel dominates the whole rainbow pattern and the outer rainbow can only be seen in the magnified inset. The experimental result shown in Fig. 4 agrees well with the above predictions of a very weak outer rainbow, since for $j \geq 3$ no population of the final levels has been found. Because of the limited resolution of the experiment no further details of the outer rainbow have been observed and therefore the experimental values are not shown in the inset.

Finally, electron-CO collisions are investigated. In this case, both rainbows are quite close together which may be seen from the ratio

$$\frac{J_R^{(1)}}{J_R^{(2)}} = \frac{r_1}{r_2} = \frac{m_2}{m_1} \approx \frac{3}{4}. \quad (18)$$

Since the charge of the carbon nucleus is $6e$ and the charge of the oxygen nucleus is $8e$, the outer rainbow

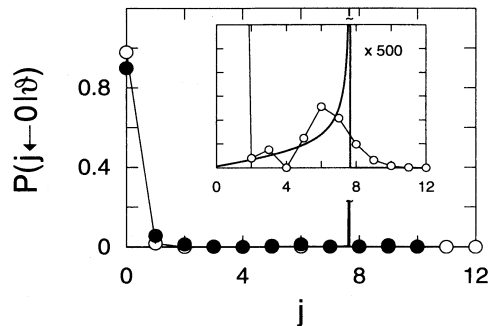


FIG. 4. For two energies and two angles, the experimental results (●) of electron-HCl scattering are compared with the predictions of the spectator model (—○—) and the classical rainbow distribution (—). The inset shows a magnification of the outer rainbow region.

corresponding to scattering from the carbon atom is only slightly weaker than the contribution caused by the electron-oxygen collision. As discussed above, for this case a breakdown of the Coulomb-scattering approximation should be clearly observable at small scattering angles. The condition (14) for applicability of the Coulomb approximation may be approximately fulfilled for an impact energy of 200 eV and scattering angles larger than 120° , i.e., for values of $a_0 \Delta k$ of about 7. As demonstrated in Fig. 5, the rainbow patterns predicted by the spectator model within the Coulomb-scattering approximation agree quite well with the experimental results for a collision energy of 200 eV and large scattering angles. For scattering angles larger than 140° the double rainbow structure is well resolved, but for decreasing angles both quantum rainbow maxima overlap, forming a single pronounced maximum. Additionally, larger differences between experiment and the above theory appear for decreasing scattering angles. The same effect

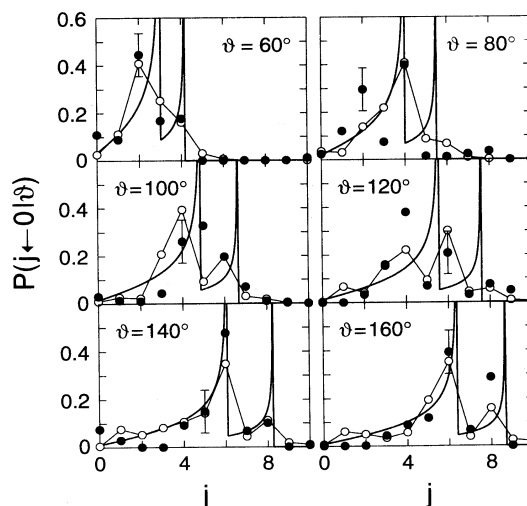


FIG. 5. Experimental results (●) of electron-CO scattering in comparison with the predictions of the quantum (—○—) and classical (—) spectator model for an impact energy of 200 eV and various scattering angles ϑ .

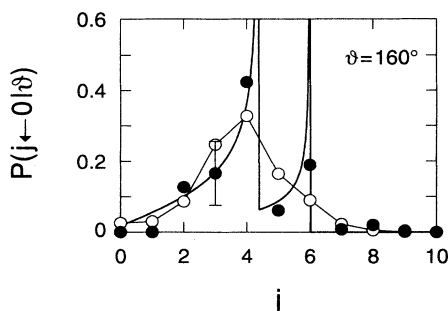


FIG. 6. Experimental rotational transition probabilities (\bullet) in electron-CO scattering in comparison with the quantum ($\text{---}\circ\text{---}$) and classical ($\text{---}\bullet\text{---}$) spectator model for an impact energy of 100 eV and a scattering angle of 160° .

has been found for lower energies such as 100 eV, where even for large scattering angles the Coulomb approximation breaks down. This can be seen in Fig. 6.

Here, we can conclude that for $a_0\Delta k \geq 7$ the Coulomb

approximation leads to quite reliable transition probabilities at fixed scattering angle. Note, however, that for prediction of the absolute values of the differential cross sections in electron-molecule collisions, the condition (14) requires much higher $a_0\Delta k$ values.

V. SUMMARY

State-resolved differential cross sections for rotational transitions in electron-molecule collisions at intermediate collision energies ($\sim 10^2$ eV) for N_2 , Cl_2 , HCl , and CO molecules revealed pronounced rotational rainbow structures similar to the Na_2 scattering results reported previously. These rainbow structures may therefore be considered as a general phenomenon in electron-molecule scattering. In all cases, the two-center scattering model using an additional Coulomb-scattering approximation was found to provide an extremely good quantitative description of the rotational transition probabilities.

-
- [1] G. Ziegler *et al.*, Phys. Rev. Lett. **58**, 2642 (1987); Z. Phys. D **16**, 207 (1990).
 [2] G. Ziegler, S. V. K. Kumar, P. Dittmann, and K. Bergmann, Z. Phys. D **10**, 247 (1988).
 [3] H. J. Korsch and A. Ernesti, J. Phys. B **25**, 3565 (1992).
 [4] H. J. Korsch, in *The Physics of Electronic and Atomic Collisions*, edited by T. Andersen *et al.*, AIP Conf. Proc. No. 295 (AIP, New York, 1993), pp. 339–349.
 [5] H. D. Meyer, Phys. Rev. A **34**, 1797 (1986).
 [6] H. J. Korsch, H. Kutz, and H. D. Meyer, J. Phys. B **20**, L433 (1987).
 [7] H. J. Korsch, H. D. Meyer, and C. P. Shukla, Z. Phys. D **15**, 227 (1990).
 [8] S. V. K. Kumar *et al.*, Phys. Rev. A **44**, 268 (1991).
 [9] A. Ernesti and H. J. Korsch, Phys. Rev. A **44**, 4095 (1991).
 [10] A. Ernesti and H. J. Korsch, Europhys. Lett. **16**, 433 (1991); Z. Phys. D **27**, 173 (1993); **32**, 101 (1994).
 [11] A. Ernesti and H. J. Korsch, Z. Phys. D **16**, 201 (1990).
 [12] A. Ernesti and H. J. Korsch, J. Phys. B **23**, L379 (1990); **24**, 1877 (1991); **26**, 4257 (1993).
 [13] A. Ernesti, J. Phys. B **27**, 4735 (1994).
 [14] D. J. Kouri, in *Atom-Molecule Collision Theory—A Guide for the Experimentalist*, edited by R. B. Bernstein (Plenum, New York, 1979), Chap. 9.
 [15] L. D. Landau and E. M. Lifschitz, *Quantum Mechanics* (Pergamon Press, New York, 1977).
 [16] H. Friedrich, *Theoretical Atomic Physics* (Springer, New York, 1991).
 [17] I. Shimamura, Chem. Phys. Lett. **73**, 328 (1980).
 [18] M. Gote, Ph.D. thesis, Universität Kaiserslautern, 1994.
 [19] M. Gote and H. Ehrhardt, J. Phys. B (to be published).
 [20] H. Kutz, Ph.D. thesis, Universität Heidelberg, 1994.
 [21] H. Kutz and H. D. Meyer, Phys. Rev. A **51**, 3819 (1995).